JOURNAL OF CATALYSIS 106, 401–409 (1987)

The Enhancement of CO Hydrogenation on Rhodium by TiO_x Overlayers

M. E. LEVIN,*,§ M. SALMERON,† A. T. BELL,*,†,§,[1] AND G. A. SOMORJAI*,†,‡

*Materials and Molecular Research Division and †Center for Advanced Materials, Lawrence Berkeley Laboratory; and Departments of ‡Chemistry and §Chemical Engineering, University of California, Berkeley, California 94720

Received January 27, 1987; revised March 17, 1987

The kinetics of CO hydrogenation at atmospheric pressure over a polycrystalline Rh foil with titania deposits were characterized with respect to the surface composition. The titania overlayers (TiO_x, $x \sim 1.9$) were prepared by titanium evaporation under ultrahigh vacuum with subsequent oxidation. Coverages were determined by Auger electron spectroscopy (AES). A sharp maximum in methanation activity, relative to the clean Rh surface, was observed with coverage. A threefold enhancement in activity was found for a TiO_x coverage of 0.15 of a monolayer. The increase in rate at low coverages was accompanied by a higher selectivity toward olefins (10% → 31%), a lower activation energy (24.4 → 16.8 kcal/mol), a higher H_2 reaction order (1.0 → 2.6), and a higher CO reaction order (−1.0 → −0.3). The kinetic parameters for olefin production were noticeably different than those for paraffin production as well. The dependence of the activity on TiO_x coverage has been modeled through a Monte Carlo simulation assuming the existence of sites of high activity at the oxide–metal interface. This model is consistent with the premise of Ti^{3+} participation in the dissociation of CO.

1. INTRODUCTION

It has been established by various authors (see, for example, Refs. (*1–4*)) that the hydrogenation of CO over Group VIII metals supported on titania proceeds more rapidly than when these metals are supported on silica or alumina. A growing body of work (*5–10*) suggests that the higher activity of titania-supported catalysts is attributable to the migration of reduced titania (TiO_x) species onto the surface of the supported metal particles. This view is further supported by recent evidence that the catalytic properties of TiO_2-promoted Pt-black, Pd/SiO_2, and Rh/SiO_2 resemble those of TiO_2-supported Pt, Pd, and Rh (*11–13*).

To better understand the effects of TiO_x surface species overlayers, studies have been undertaken using metal foils and single crystals. Demmin *et al.* (*14*) observed an increase in the activity for CO hydrogenation when titania was deposited on a Pt foil, as well as a 10 kcal/mol decrease in the activation energy. Chung and co-workers (*15*) measured the reaction rate on a Ni(111) surface as a function of TiO_x coverage. They found a sharp maximum at 7.5% of a monolayer (ML) of TiO_x representing a fivefold increase in methanation activity. An increase in olefin formation in the presence of TiO_x was also observed.

The objective of the present study was to investigate the effects of TiO_x species on the activity and selectivity of CO hydrogenation over a Rh foil. Titania surface coverages of less than 0.30 ML were found to enhance significantly the rates of hydrocarbon formation, and, in particular, the synthesis of olefins. Investigations of the reaction kinetics revealed that, in addition, TiO_x surface species strongly influence the rate parameters associated with each product. A preliminary discussion of the data

[1] To whom correspondence should be addressed.

0021-9517/87 $3.00

for methane formation is given in Ref. (*16*). Reported here are the effects of TiO_x species on the kinetics of forming C_{2+} hydrocarbons. These results are discussed together with those for methane in the light of a proposed model for interpreting the effects of TiO_x promotion.

2. EXPERIMENTAL

A diffusion-pumped ultrahigh vacuum (UHV) chamber with a base pressure of less than 2×10^{-9} Torr was employed in this investigation. As described in our previous work (*17*), this chamber housed an Auger electron spectrometer, a quadrupole mass spectrometer, and an atmospheric pressure isolation cell. The isolation cell provided the capability to enclose the sample and to carry out a reaction while the rest of the chamber remained under vacuum.

Titanium was vapor-deposited onto a clean Rh foil (1 cm^2, 0.003 in. thickness, and 99.8% purity) by resistively heating a Ti-wrapped tungsten filament in a manner similar to the sample preparation in our chemisorption work (*17*). The Rh foil was mounted on 0.030-in. Pt support wires. *In vacuo* oxidation (2×10^{-6} Torr O_2 at 623 K) was found to be sufficient for oxidizing the Ti overlayer to near-stoichiometric TiO_x, where $x \sim 1.9 \pm 0.15$. Excess oxygen bound to the Rh was then removed as CO_2 by repeated exposures to CO and heating to 773 K. The TiO_x coverage was monitored at three points on each face of the foil by Auger electron spectroscopy (AES) to ensure uniform deposition.

The monolayer coverage was determined from a plot of the normalized AES peak intensities for Rh, Ti, and O as a function of Ti dosing time (*17*). The TiO_x overlayer grows in a two-dimensional manner until near-completion of the monolayer, followed by three-dimensional growth (i.e., Stranski–Krastanov growth). Monolayer coverage for the TiO_x/Rh system occurs when the Rh signal is attenuated to 34% of its initial intensity. This value of the attenuation coefficient seems to indicate a bilayer structure of the titania.

The low surface area of the sample (2×1 cm^2) necessitated operating reactions in a batch mode. The total reactor loop volume including the cell plus the circulation loop was 125 cm^2. Gases were circulated through the loop by a metal bellows pump at a rate of about 200 cm^3/min, as monitored with a rotameter.

A six-port sampling valve with a 0.25-cm^3 sampling loop permitted periodic removal of a small portion of the reaction gas mixture for analysis. Hydrocarbons were separated and analyzed with a Hewlett–Packard Model 1920A gas chromatograph equipped with a flame ionization detector. A 6-ft column packed with Porapak N and held at 328 K separated all hydrocarbon products easily.

The reactions were performed at a total pressure of 1 atm. After passing through a cold trap to condense out metal carbonyls, carbon monoxide was introduced into the loop to a pressure of 0.33 atm. Hydrogen was passed through a liquid nitrogen trap and added to the loop to bring the total pressure to 1 atm. In the partial pressure dependence studies, where the sum of the H_2 and CO partial pressures was less than 1 atm, the total pressure in the loop was brought to 1 atm by filling with argon.

The reaction gas mixture was circulated for 20 min prior to a reaction, with the catalyst remaining at room temperature. During this time, samples of the gas mixture were analyzed to determine if any hydrocarbons were initially present or if the reaction was already proceeding. A gas sample was taken 5 min after heating of the foil began and subsequent samples were taken at 10- to 15-min intervals. After 1–2 h of reaction, the foil was allowed to cool and no additional reactivity was observed. Following each reaction, the gas chromatograph was calibrated with a 1% CH_4/Ar mixture. Reaction rates for each product were calculated from the initial slopes of product accumulation-versus-time plots.

These rates remained constant during the first 30–40 min of each run before slowly decaying due to carbon buildup on the surface.

Evacuation of the reaction loop followed the completion of a reaction. This was accomplished with a rotary-vane mechanical pump followed by a sorption pump. When the reaction cell was adequately pumped, it was opened to the UHV chamber to allow sample characterization by AES.

3. RESULTS

Displayed in Fig. 1 is the methane production rate from CO and H_2 for varying TiO_x coverages. Reaction rates were measured at a temperature of 553 K, and at H_2 and CO partial pressures of 0.67 and 0.33 atm, respectively. With the addition of small amounts of TiO_x (<0.15 ML) to the clean Rh surface, a sharp rise in reaction rate is noted. At the maximum corresponding to 0.15 ML TiO_x, a threefold increase in rate is observed. Beyond this coverage, the rate decreases rapidly to a coverage of about 0.30 ML and more slowly for higher TiO_x coverages. The residual methanation activity at monolayer coverage could be reduced by increasing the TiO_x coverage further. A gold foil mounted on the Pt support wires, in place of the Rh sample, showed negligible activity under identical reaction conditions, indicating an insignificant contribution to the reaction rate by the support wires or reaction cell walls.

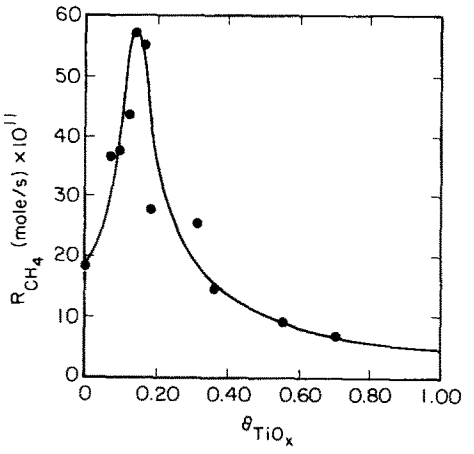

FIG. 1. Methanation rate on TiO_x/Rh as a function of TiO_x coverage. Reaction conditions were 553 K, 1 atm total pressure, and a H_2:CO ratio of 2:1.

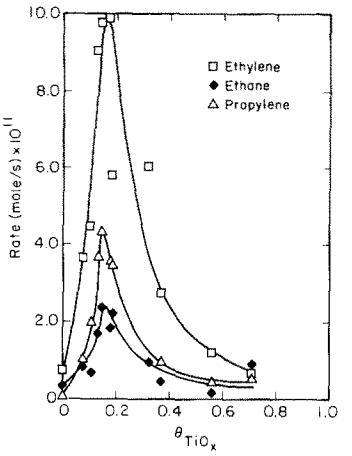

FIG. 2. Higher hydrocarbon formation rates on TiO_x/Rh as a function of TiO_x coverage. Reaction conditions were 553 K, 1 atm total pressure, and a H_2:CO ratio of 2:1.

The effect of prereduction of the sample on the methanation rate was also investigated. Prior to reaction, the TiO_x/Rh sample was heated in 50 Torr H_2 at 753 K for 5 min. For five different titania coverages, hydrogen pretreatment was found to have no significant effect on the methanation rate.

More dramatic enhancements are observed in the formation of C_2 and C_3 hydrocarbons at low coverages as seen in Fig. 2. Most notable are the more than order-of-magnitude increases in rates for ethylene and propylene. As in the case of methane formation, the rates reach maxima around 0.15 ML TiO_x and thereafter decrease rapidly with increasing titania coverage. Product selectivities are shown in Fig. 3. The methane content of the hydrocarbon product falls from a value of 94 mol% when no titania is present to nearly 60 mol% for $\theta_{TiO_x} = 0.20$. Ethylene and propylene are the predominant higher hydrocarbon species comprising roughly 34 mol% of the total hydrocarbon product. At

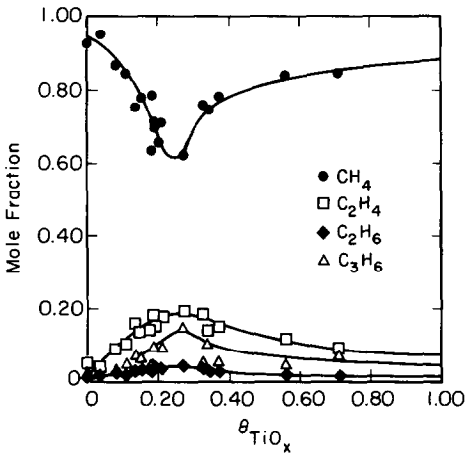

FIG. 3. Hydrocarbon product selectivity as a function of TiO_x coverage.

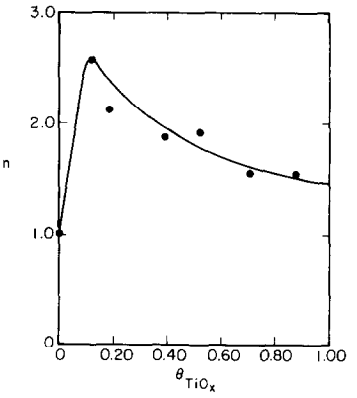

FIG. 5. Hydrogen partial pressure dependence as a function of TiO_x coverage. Reaction conditions were identical to those for Fig. 1 except the hydrogen partial pressure was varied from 0.23 to 0.67 atm.

higher coverages, the selectivities return to values more characteristic of clean Rh.

The influence of TiO_x on the kinetic parameters (activation energy and reactant partial pressure dependences) of CO hydrogenation on Rh was investigated for temperatures between 473 and 633 K, H_2 partial pressures between 0.23 and 0.67 atm, and CO partial pressures between 0.037 and 0.33 atm. The observed rate of methane formation, R_{CH_4}, was described with the power law expression

$$R_{CH_4} = k_0 \exp\left(-\frac{E_A}{RT}\right) p_{H_2}^n p_{CO}^m, \quad (1)$$

where the temperature and partial pressures are represented by T and p_{H_2} and p_{CO}, respectively. The variations of the activation energy (E_A), and the H_2 and CO partial pressure dependences (n and m, respectively) are shown in Figs. 4–6. The plot of activation energy versus coverage (Fig. 4) shows a minimum of 16.8 ± 0.5 kcal/mol at a coverage just above 0.2 ML. This represents a downward change of about 7.7 kcal/mol from the value of E_A for clean Rh.

The hydrogen partial pressure dependence displayed in Fig. 5 rises sharply from a value of 1.0 ± 0.1 for clean Rh to 2.6 ± 0.1 at $\theta_{TiO_x} = 0.10$ and then slowly decays to

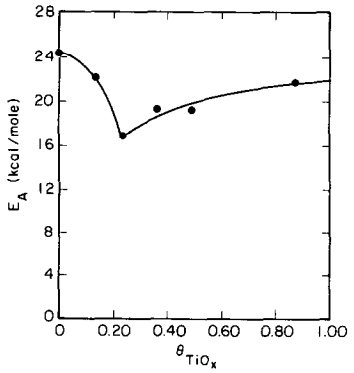

FIG. 4. Activation energy for methane formation as a function of TiO_x coverage. Reaction conditions were identical to those for Fig. 1 except the temperature was varied between 473 and 633 K.

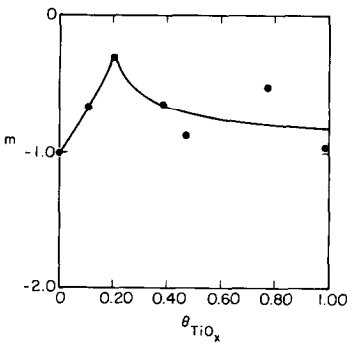

FIG. 6. CO partial pressure dependence as a function of TiO_x coverage. Reaction conditions were identical to those for Fig. 1 except the CO partial pressure was varied between 0.037 and 0.33 atm.

a value of 1.5 near monolayer coverage. This trend is repeated in the CO partial pressure dependence plot (Fig. 6), but to a lesser extent. The CO order passes through a maximum at $\theta_{TiO_x} = 0.15$ with $m = -0.3 \pm 0.1$, compared with -1.0 ± 0.1 for clean Rh.

The kinetic parameters for higher hydrocarbon formation were also determined with power law expressions of the form of Eq. (1) and the parameter values are plotted in Figs. 7–9. As in the case for methane, a decrease in the activation energy at low coverages is observed for ethane (Fig. 7), followed by a gradual rise in the activation energy above 0.30 ML. However, the presence of TiO_x has virtually no effect on the activation energies of ethylene and propylene.

For all three hydrocarbons, the H_2 reaction orders increase significantly between 0 and 0.10 ML (Fig. 8). Ethane appears to follow the same trend as methane; the olefins rise from near zero-order dependence to 1.5 order and fall slightly thereafter. The trends for the CO reaction orders are particularly interesting. Unlike methane, where a -1.0 order is observed, positive orders between 0.5 and 1.5 are seen for the other hydrocarbons on the clean surface (Fig. 9). With the addition of titania, the CO reaction orders for the C_{2+} hydrocarbons decrease to -1.0. Propylene, though, exhibits a broad minimum at about 0.40 ML where the reaction becomes zero order in CO.

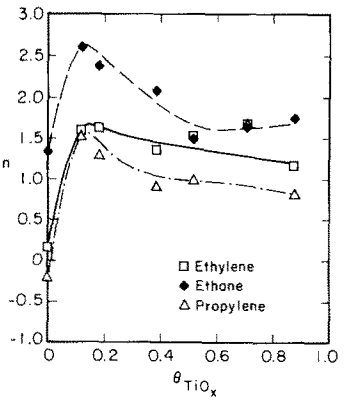

FIG. 8. Hydrogen partial pressure dependence for higher hydrocarbon formation as a function of TiO_x coverage.

4. DISCUSSION

4.1 Methane Formation

As indicated in Fig. 1, a clear enhancement in methanation activity occurs for TiO_x coverages less than 0.30 ML while at higher coverages the rate diminishes gradually to a level well below that for clean Rh. Similar behavior has been observed by Chung *et al.* (*15*) for TiO_x deposited on a Ni(111) surface and increases in activity of Pt foil (*14*), Pt-black (*11*), SiO_2-supported

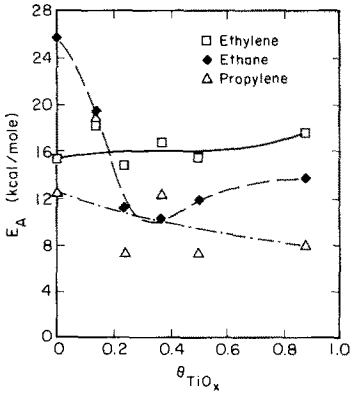

FIG. 7. Activation energy for higher hydrocarbon formation as a function of TiO_x coverage.

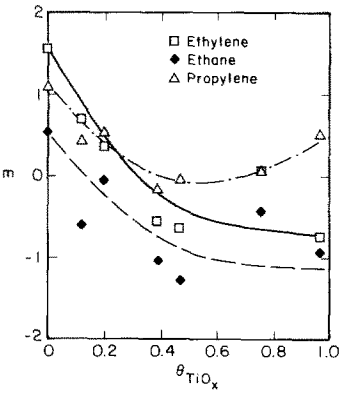

FIG. 9. CO partial pressure dependence for higher hydrocarbon formation as a function of TiO_x coverage.

Pd (*12*), and SiO_2-supported Rh (*13*) have been reported upon promotion with TiO_x.

It is apparent from Figs. 4–6 that at TiO_x coverages comparable to those where R_{CH_4} reaches a maximum, the value of E_A is smaller, and the values of m and n are larger compared to the values of these parameters for clean Rh. A reduction in E_A has also been reported by Demmin *et al.* (*14*) for a TiO_x-promoted Pt foil and by Rieck and Bell (*12*) for TiO_x-promoted Pd/SiO_2. A sharp increase in hydrogen order was also observed by Vannice (*18*) for TiO_2-supported Rh in comparison with Al_2O_3-supported Rh, while only a slight change in the CO partial pressure dependence was found.

The influence of TiO_x on the CO hydrogenation activity of Group VIII metals has been attributed to Ti^{3+} ions present at the perimeter of small TiO_x islands decorating the metal surface (*19–26*). For a TiO_x-promoted Pt foil, Dwyer *et al.* (*27*) detected a substantial concentration of Ti^{3+} species by X-ray photoelectron spectroscopy (XPS). XPS studies conducted in our own laboratory (*28*) have shown that the percentage of Ti^{3+} formed by either CO or H_2 reduction increases with lower TiO_x coverage. Since the perimeter-to-area ratio of overlayer islands also rises with lower TiO_x coverages, these results suggest that Ti–O bonds near the periphery of TiO_x islands are more prone to attack by reducing agents chemisorbed on the Rh metal. The oxygen-deficient Ti^{3+} species along the oxide island periphery may then interact with the oxygen end of CO adsorbed on nearby metal sites, as shown in Fig. 10. When CO is adsorbed on Rh sites adjacent to the Rh–Ti boundary, the C=O bond is long enough for the oxygen to reach the Ti^{3+} ion. The acid–base interaction between CO and the oxophilic Ti^{3+} should enhance the dissociation of CO—an essential step in the formation of methane.

To explain the observed methanation rate dependence on TiO_x coverage, we can propose that an ensemble of Ti^{3+} and Rh

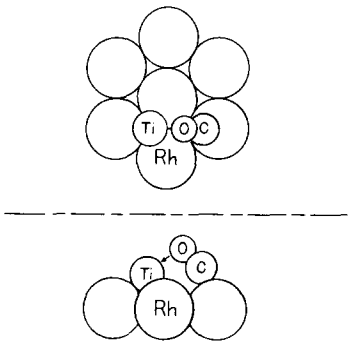

FIG. 10. A schematic for possible bonding between CO and peripheral Ti^{3+} sites.

sites near the periphery of the islands are the active sites where an enhancement in rate occurs. The simplest ensemble that can be considered would include a single Rh site at the periphery. To determine the number of Rh atoms at the titania island periphery, we have employed a Monte Carlo simulation of TiO_x island growth around fixed nucleation sites. This simulation has been used to model the suppression in CO chemisorption at room temperature on TiO_x/Rh (*17*). By excluding CO chemisorption at Rh sites bordering TiO_x islands, excellent agreement between the model and experimental data was found for a nucleation site density of 4.5×10^{13} cm^{-2} (~3% site density). Calculations were performed for a 100×100 hexagonal array.

With the nucleation site density determined from the chemisorption modeling, counting the number of these "peripheral" rhodium sites by use of the Monte Carlo simulation produces a function reaching a maximum at $\theta_{TiO_x} \approx 0.35$ ML, corresponding to the maximum chemisorption suppression at low pressures (*17*). Neither the position of the maximum nor the shape of the curve agrees with the trend of the experimental data.

A model which does give agreement with the observed trends is one in which a site pair consisting of a "peripheral" Rh site and an adjacent, non-"peripheral" Rh site has an intrinsically higher methanation activity. If it is assumed that the contribu-

tion of these peripheral site pairs to the total methanation rate is proportional to the product of the surface concentrations of each constituent site, then the total methanation rate in this model becomes (*16*)

$$R_{CH_4} = S_T \left[\left(\frac{n_0}{n_T} \right) r_0 + \left(\frac{n_p}{n_T} \right) \left(\frac{n_{p'}}{n_T} \right) r_{pp'} \right], \quad (2)$$

where r_0 and $r_{pp'}$ represents the intrinsic methanation rates per unit catalyst area for the Rh sites unaffected by TiO_x and the highly active site pairs near the perimeter of the TiO_x islands, respectively. The numbers of each type of site present—exposed, peripheral, adjacent to peripheral, and total–are given by n_0, n_p, $n_{p'}$, and n_T, respectively.

The number densities of the various types of site at various TiO_x coverages were determined through use of the Monte Carlo simulation. The values of n_0, n_p, and $n_{p'}$ were combined with the experimentally observed reaction rate for clean Rh, r_0, in Eq. (2) to yield the total reaction rate as a function of coverage. The value of $r_{pp'}$ was chosen so that the maximum value of the predicted rate agrees with the maximum in the observed methanation rate. For this condition to be met, $r_{pp'}/r_0 = 43$. The dependence of the calculated rate on the TiO_x coverage, described by Eq. (2), is shown in Fig. 11 (solid curve), along with the experimental points presented in Fig. 1 for comparison. Good agreement is seen between the location of the predicted rate maximum and that of the experimental data. The width of the calculated peak though is broader than that exhibited by the data.

Another feature of this model is that it accounts for the extrema in kinetic parameters observed in Figs. 4–6. At low coverages (≤0.3 ML), the rate is dominated by the reaction occurring at the TiO_x/Rh interface, as reflected by the changes in activation energy and partial pressure dependences. At higher coverages, this contribution diminishes rapidly until kinetics typifying CO hydrogenation on clean Rh dominate.

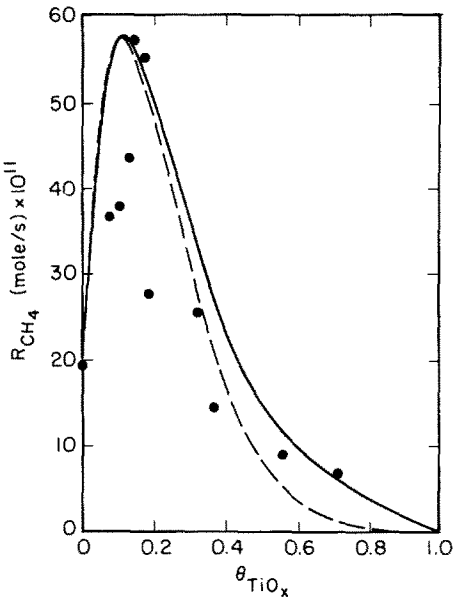

FIG. 11. A comparison between the predicted methanation rate and the experimental data as a function of TiO_x coverage. The solid line denotes the calculated rate for peripheral Rh sites active for both the Ti^{3+}-assisted reaction pathway and the normal reaction pathway on bare Rh. The dashed line represents the calculated rate if the peripheral Rh sites only participate in the Ti^{3+}-assisted reaction pathway.

At coverages approaching one monolayer, virtually all exposed surface Rh atoms border TiO_x islands. These Rh sites may catalyze CO hydrogenation either through the mechanism normally occurring on Rh metal or through the Ti^{3+}-assisted pathway, depending on the prevalence of Ti^{3+} species at the metal/oxide interface under reaction conditions. The number of sites, n_0, catalyzing the reaction through the normal CO hydrogenation mechanism on bare Rh is therefore taken to be the total number of exposed Rh atoms.

In an earlier publication (*16*), n_0 was taken as the number of Rh atoms that could chemisorb CO at low pressures. The plot of predicted rate versus TiO_x in this case is depicted by the dashed curve in Fig. 11. However, with n_0 defined in this manner,

the model does not predict the extrema in kinetic parameters of Figs. 4–6.

Through bonding with the oxygen in CO, Ti^{3+} is oxidized to the 4+ oxidation state. Regeneration of the Ti^{3+} site must occur for this reaction pathway to be followed again. One scheme for the reduction of Ti^{4+} back to Ti^{3+} is given below:

1. Ti^{4+}—O—M + H(a) $\rightleftharpoons$ Ti^{4+}—OH (M = Rh or Ti^{4+})
2. Ti^{4+}—OH + H(a) $\rightleftharpoons$ Ti^{3+} + H_2O

The high reaction order of 2.6 with respect to hydrogen in the Ti^{3+}-assisted reaction pathway suggests that five or six hydrogenation steps are crucial in determining the overall reaction rate; Reactions 1 and 2 comprise two of these steps. In contrast, for bare Rh, where CO dissociation is believed to be rate-determining, the first-order H_2 dependence suggests that only two hydrogenation steps are important. Consequently, changes in the abundance of hydrogen on the surface are expected to affect the Ti^{3+}-assisted methanation rate to a greater extent.

As higher TiO_x coverages are reached, there is a reduction in the number of exposed non-peripheral sites relative to the number of peripheral Rh sites. Furthermore, the high dispersion of the oxide overlayer serves to break up Rh–Rh pairs necessary for the chemisorption and dissociation of molecular hydrogen. The supply of surface hydrogen decreases rapidly with coverage and the impact on the Ti^{3+}-assisted reaction pathway, where the H_2 partial pressure dependence is nearly cubic, is much greater than on the normal pathway, where the dependence is only linear. At the microscopic level, this means that at near-monolayer coverages, there is insufficient surface hydrogen to maintain the Ti^{3+}-assisted reaction rate and so the slower pathway, in which CO dissociation is rate-determining, is the principal contributor.

The absence of any effect by prereduction of the sample upon reaction rate, as observed in this study and others (*20, 29–31*), may be related to the active role of Ti^{3+} species in CO hydrogenation. Whether preoxidized or prereduced, the oxidation state (and perhaps also the morphology) of the oxide overlayer may be determined by the reaction conditions, where both H_2 and H_2O are present. In particular, the percentage of Ti^{3+} after reaction was found to be only weakly dependent on the pretreatment conditions (*28*).

4.2 Formation of C_{2+} Hydrocarbons

Comparison of Figs. 7–9 with Figs. 4–6 shows two principal patterns: (1) the kinetics of ethane formation are similar to those of methane formation and (2) the kinetics of ethylene and propylene formation are likewise similar. Significant differences are seen only in the case of the CO partial pressure dependence (e.g., −1.0 order for CH_4 and +0.5 order for C_2H_4) and these can be attributed to the requirement of additional surface carbon to form large hydrocarbons. Of particular interest is the difference in hydrogen partial pressure dependences between paraffins and olefins. The methane and ethane hydrogen orders are between $\frac{1}{2}$ and 1 greater than those for ethylene and propylene. Similar behavior was noted by Dictor and Bell (*32*) for unsupported Fe and by Kellner and Bell (*33*) for Al_2O_3-supported Ru. In both of these studies, a difference in order of roughly $\frac{1}{2}$ was seen between paraffins and olefins.

5. CONCLUSIONS

An enhancement in CO hydrogenation activity was observed upon deposition of TiO_x onto a polycrystalline Rh foil. The methanation rate passed through a maximum at 0.15 ML TiO_x, corresponding to a threefold increase in rate, and was accompanied by maxima in the ethylene and propylene production rates. The activation energy and reactant partial pressure dependences also exhibited extrema at low

TiO_x coverages while at high TiO_x coverages they displayed behavior characteristic of bare Rh metal. The olefins exhibited different kinetic parameters than the paraffins. The modification of the catalytic properties of rhodium by titania has been attributed to participation by Ti^{3+} species at the metal–oxide interface in the CO dissociation step. A Monte Carlo simulation gives good quantitative agreement between the experimental data and a model invoking two-site ensembles along the TiO_x island periphery.

ACKNOWLEDGMENTS

We are grateful to Kevin J. Williams and Howard Chu for their assistance in performing experiments. This work was supported by the Office of Basic Energy Sciences, Chemical Sciences Division of the U.S. Department of Energy under Contract DE-AC03-76SF00098.

REFERENCES

1. Bell, A. T., "Supports and metal–support interactions in catalyst design," *in* "Catalyst Design–Progress and Perspectives" (L. L. Hegedus, Ed.). Wiley, New York, 1987.
2. Katzer, J. R., Sleight, A. W., Gajardo, P., Michel, J. B., Gleason, E. F., and McMillan, S., *Faraday Discuss.* **72,** 121 (1981).
3. Orita, H., Naito, S., and Tamaru, K., *J. Chem. Soc. Chem. Commun.* **18,** 993 (1983).
4. Haller, G. L., Henrich, V. E., McMilland, M., Resasco, D. E., Sadeghi, H. R., and Sakellson, S., *in* "Proceedings, 8th International Congress on Catalysis," Vol. V, p. 135. Berlin, 1984.
5. Santos, J., Phillips, J., and Dumesic, J. A., *J. Catal.* **81,** 147 (1983).
6. Resasco, D. E., and Haller, G. L., *J. Catal.* **82,** 279 (1983).
7. Sadeghi, H. R., and Henrich, V. E., *J. Catal.* **87,** 279 (1984).
8. Takatani, S., and Chung, Y.-W., *J. Catal.* **90,** 75 (1984).
9. Belton, D. N., Sun, Y.-M., and White, J. M., *J. Phys. Chem.* **88,** 5172 (1984).
10. Baker, R. T. K., Chludzinski, J. J., and Dumesic, J. A., *J. Catal.* **93,** 312 (1985).
11. Dwyer, D. J., Robbins, J. L., Cameron, S. D., Dudash, N., and Hardenbergh, J., *in* "Strong Metal Support Interaction" (R. T. K. Baker, S. J. Tauster, and J. A. Dumesic, Eds.), ACS Symposium Ser. No. 298, p. 21. Amer. Chem. Soc., Washington, DC, 1986.
12. Rieck, J. S., and Bell, A. T., *J. Catal.* **99,** 262 (1986).
13. Pande, N. K., Ph.D. thesis, University of California, Berkeley.
14. Demmin, R. A., Ko, C. S., and Gorte, R. J., *J. Phys. Chem.* **89,** 1151 (1985).
15. Chung, Y.-W., Xiong, G., and Kao, C.-C., *J. Catal.* **85,** 237 (1984).
16. Levin, M. E., Salmeron, M., Bell, A. T., and Somorjai, G. A., *Faraday Symp. Chem. Soc.* **21,** paper 10 (1986).
17. Levin, M., Salmeron, M., Bell, A. T., and Somorjai, G. A., *Surf. Sci.* **169,** 123 (1986).
18. Vannice, M. A., *J. Catal.* **74,** 199 (1982).
19. Burch, R., and Flambard, A. R., *J. Catal.* **78,** 389 (1982).
20. Bracey, J. D., and Burch, R., *J. Catal.* **86,** 384 (1984).
21. Anderson, J. B. F., Bracey, J. D., Burch, R., and Flambard, A. R., *in* "Proceedings, 8th International Congress on Catalysis," Vol. V, p. 111. Berlin, 1984.
22. Vannice, M. A., and Sudhakar, C., *J. Phys. Chem.* **88,** 2429 (1984).
23. Sudhakar, C., and Vannice, M. A., *J. Catal.* **95,** 227 (1985).
24. Sachtler, W. M. H., *in* "Proceedings, 8th International Congress on Catalysis," Vol. V, p. 151. Berlin, 1984.
25. Sachtler, W. M. H., Shriver, D. F., Hollenberg, W. B., and Long, A. F., *J. Catal.* **92,** 429 (1985).
26. Rieck, J. S., and Bell, A. T., *J. Catal.* **96,** 88 (1985).
27. Dwyer, D. J., Cameron, S. D., and Gland, J., *Surf. Sci.* **159,** 430 (1985).
28. Levin, M. E., Salmeron, M., Bell, A. T., and Somorjai, G. A., to be published.
29. Solymosi, F., Tombácz, I., and Kocsis, M., *J. Catal.* **75,** 78 (1982).
30. Vannice, M. A., Twu, C. C., and Moon, S. H., *J. Catal.* **82,** 213 (1983).
31. Morris, S. R., Moyes, R. B., and Wells, P. B., *in* "Studies in Surface Science and Catalysis" (B. Imelik *et al.*, Eds.), Vol. 11, p. 247. Elsevier, Amsterdam, 1982.
32. Dictor, R. A., and Bell, A. T., *Appl. Catal.* **20,** 145 (1986).
33. Kellner, C. S., and Bell, A. T., *J. Catal.* **70,** 418 (1981).